TECHNICAL PAPER

Multi-stage single-point incremental forming: an experimental investigation of thinning and peak forming force

Nikhil Bari[1] · Shailendra Kumar[1]

Abstract

Multi-stage single-point incremental forming (MSPIF) is used to form sheet metal parts of complex geometry with steep wall angles. The present paper describes an experimental investigation focused on part thinning and peak forming force acting on part formed by MSPIF. Four parameters, namely step depth, tool diameter, sheet thickness and initial wall angle, are considered to study their influence on part thinning and vertical component of forming force. Experiments are designed on the basis of central composite design of response surface methodology, and results are analyzed using analysis of variance. It is found that initial wall angle is the most significant parameter for thinning followed by sheet thickness. Thinning decreases with decrease in initial wall angle and increase in sheet thickness. For peak forming force, sheet thickness is found most significant parameter followed by tool diameter, step depth and initial wall angle. It decreases with decrease in all four process parameters. Further, regression models of thinning and forming force are developed. Optimization of process parameters is also performed to minimize thinning and forming force.

Keywords Multi-stage single-point incremental forming · Sheet metal · Thinning · Forming force · Process parameters · Optimization

1 Introduction

Single-point incremental forming (SPIF) is a flexible sheet metal forming process, in which the required shape is formed using incremental steps. This process is also called as die-less process as it does not require tool and punch, which also reduces lead time and effective tooling cost. SPIF is increasing its adaptability in industry to create customized products [1]. In SPIF, it is difficult to form parts with steeper wall angle. The failure of parts formed by SPIF process is mostly caused by uneven thickness distribution and excessive localized thinning [2]. Therefore, it is difficult to form complex products with high wall angle. SPIF process can be performed in single or multiple stages. In single-stage SPIF, sheet is formed to desired shape in one pass, while, in multi-stage single-point incremental forming (MSPIF), final shape is obtained using more number of passes [2]. In MSPIF process the sheet is continuously deformed by increasing wall angles (or drawing heights) to fabricate final shape as depicted in Fig. 1. Final wall angle (θ_f) is formed with intermediate stages of wall angles θ_1 and θ_2. In MSPIF steeper wall angles than SPIF are formed since deformation zone is extended over a larger region of the part [3–7].

To improve the thickness distribution along with formability, MSPIF method is used. Many researchers have worked on MSPIF to achieve homogeneous thickness distribution in parts. A double-pass forming approach was designed by Kim and Yang [8]. Iseki and Naganawa [9] developed a multi-stage bulging machine using spherical and cylindrical tools to form a square geometry. Filice [10] proposed an analytical model to predict the thickness distribution for final stage in MSPIF. Duflou et al. [3] developed five-stage process and compared the thickness distribution of SPIF and MSPIF process and reported that the wall thickness of MSPIF is significantly higher than that of SPIF similar results were observed by Vertbert et al. [11]. Manco et al. [12] studied the effect of different tool trajectory on thickness distribution. Li et al. [13] developed a mathematical expression to estimate

Technical Editor: Lincoln Cardoso Brandao.

✉ Shailendra Kumar
skbudhwar@med.svnit.ac.in

1 Departmental of Mechanical Engineering, Sardar Vallabhbhai National Institute of Technology, Surat 395007, India
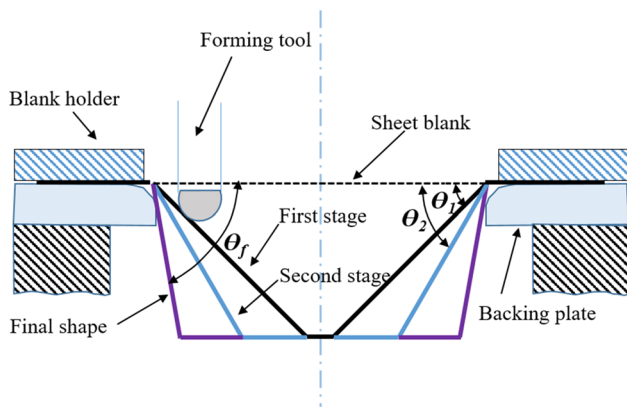
Fig. 1 Schematic of MSPIF process

Fig. 2 Length variations in MSPIF process

the necessary number of stages required to satisfy the thickness distribution. Junchao et al. [14] studied the thickness distribution of car taillight bracket formed by MSPIF process. Li et al. [15] compared the thickness distribution of parts formed by different number of stages and found that the minimum thickness increases with increasing number of forming stages; hence, uniform thickness distribution in MSPIF is observed. Liu et al. [16] compared the thickness distribution of different strategies and their combinations and found that thickness distribution depends on the initial draw angle. Cao et al. [17] developed a thickness prediction model based on nodal displacement and volume constancy. Moser et al. [18] reported that material thinning prediction is one of the major challenges in MSPIF process. Lingam et al. [19] predicted the thickness distribution of MSPIF component with mathematical modelling. This model was developed by considering plane-strain deformation with volume constancy. Otsu et al. [20] determined the strain distribution of components formed by single-stage forming and two-stage forming also compared the values with ideal sine law and reported that radial (meridian) strain of two-stage forming is influenced by angle increment per stage. Cui and Gao [21] compared the thickness distribution of different tool path strategies and concluded that variable angle straight line tool path strategy gives more uniform thickness distribution than other strategies. Ndip-et al. [22] compared the thickness distribution of each stage of seven stage geometry and reported that thickness distribution of parts made by seven stages shows uniform thickness distribution compared to parts made by single-stage forming. Zhu et al. [23] developed MSPIF toolpath strategy to get uniform thickness distribution in parts with steeper wall angle. Gohil et al. [24] generated a toolpath to form hemispherical parts.

However, some researchers have reported the limitations related to minimum thickness (thinning) of part in MSPIF process [18, 25]. Thinning in MSPIF process initiates due to rigid body motion (RBM) in MSPIF process [26]. While forming
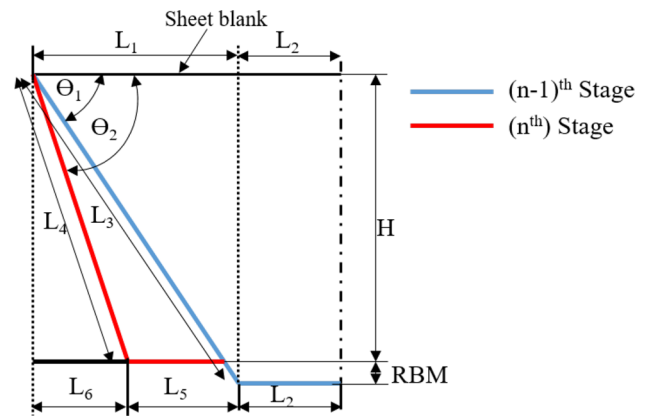
$(n+1)$th stage, the material at periphery of (nth) stage is push in downward direction and creates step-like structure at the bottom, thus reducing final wall thickness. Reasons of thinning are improper selection of material, toolpath strategy and working parameters [27].

Typical two-stage single-point incremental forming process is depicted in Fig. 2. The wall angles formed in first stage and second stage are θ_1 and θ_2, respectively. If the forming is performed for wall angle θ_2 directly, the process is single-stage forming. Conversely, if sheet is deformed to intermediated stage with wall angle θ_1 and in second stage, wall angle is changed to θ_2, the process is two (multi)-stage forming.

Let ϵ_s, and ϵ_m are the principal strains in single-stage forming and multi-stage forming, respectively [13]. According to deformation mechanism,

$$\epsilon_s = \ln \frac{l_3}{l_1} \tag{1}$$

$$\epsilon_m = \ln \frac{l_4 + l_5}{l_6 + l_5} \tag{2}$$

The strain in thickness direction (ϵ_z) [28] is obtained using,

$$\epsilon_z = -\left(\frac{\mu}{1-\mu}\right)(\epsilon_z \text{ or } \epsilon_z) \tag{3}$$

Also,

$$\ln \frac{t_f}{t_i} = \epsilon_z \tag{4}$$

Final thickness of the sheet is calculated using,

$$t_f = t_i e^{\epsilon_z} \tag{5}$$

It is clear that $\epsilon_m > \epsilon_s$, implies $(t_f)_s > (t_f)_m$; therefore, the thickness reduction in MSPIF process is higher than SPIF.

Forming force is also one of the major responses to determine power consumption, load-carrying capacity of machine, and tool life for the process. Many researchers have made efforts to study forming force in MSPIF. Ambrogio et al. [29] developed the safety monitoring system using peak force. Duflou et al. [30] experimentally investigated the effect of sheet thickness, wall angle, step depth and tool diameter on resultant force and concluded that step depth and tool diameter are significant parameter on resultant forming force. Durante et al. [31] investigated the influence of tool rotation on forming force and concluded that tool rotation has a significant effect on horizontal forces (X, Y). Aerens et al. [32] experimentally investigated the effect of sheet thickness, tool diameter, wall angle and step depth on all three components of forces and also developed the regression models for force components using different materials. Liu et al. [33] investigated the influence of sheet thickness, step depth and sheet orientation on vertical component of force and concluded that sheet orientation is the least influencing parameter on peak vertical force. Bagudanch et al. [34] experimentally investigated the effect of step depth, spindle speed, feed rate, tool diameter and sheet thickness on maximum vertical forming force of polyvinylchloride sheet and concluded that tool diameter and sheet thickness are significant parameters. Shrivastava and Tondon [35] investigated the effect of grain size on vertical component of force and reported that the increase in grain size decreases the vertical component of forming force. Kumar et al. [36] investigated and optimized the process parameters, namely, sheet thickness, step depth, tool diameter, wall angle, viscosity of oil, spindle speed and tool shape on forming forces of SPIF components and found that sheet thickness is the most influencing parameter on axial force, followed by tool diameter, tool shape and wall angle. Kumar et al. [37] studied the effect of process parameters, namely, tool diameter, wall angle and sheet thickness on maximum vertical force and reported that increase in tool diameter, sheet thickness and wall angle increases the vertical force. Gheysarian et al. [38] studied the effect of tool diameter and step depth process on average forming force. Gandla et al. [39] investigated the effect number of stages on resultant forming force and concluded as the number of stages increases, the resultant force decreases.

From the literature it is found that very less research efforts have been made to study influence of process parameters on thinning of parts and peak forming force acting in MSPIF process. There is need to investigate the quantitative effect of process parameters on these responses. The higher values of these responses are undesirable in MSPIF process. The parametric optimization is required to minimize responses simultaneously. Prediction of thinning and peak forming force is one of the key challenges in MSPIF. The present study is an attempt to fulfil the above research

gap. The objectives of present study are—(i) to investigate the effect of process parameters on percentage thinning of parts and peak forming force acting in MSPIF process, (ii) to optimize process parameters for minimizing percentage thinning and forming force, and (iii) to develop regression models for responses.

2 Experimental plan

A four-factor, three-level central composite design (CCD) is adapted to design the experiments. Step depth (A), tool diameter (B), sheet thickness (C) and initial wall angle (D) are considered as process parameters for the present study. Three levels of these parameters are coded as -1, 0 and $+1$ as given in Table 1. No categorical factor is chosen for the experiments. The levels and process parameters are selected on the basis of literature review, available experimental setup and trial experiments. Total 30 experiments with 6 experiments at center points are carried out to minimize the error.

Sheet material for the present study is aluminum 3003 alloy. The tool is made up of M2 grade high-speed high-chromium steel. The tool material is having good wear resistance property due to high-chromium content. To reduce the friction and wear, EP-90 hydraulic oil is used as lubricant. In the present work, varying wall angle–constant depth, tool path strategy is selected as it gives uniform thickness distribution compared to other strategies [40]. In all experiments, a square pyramid of $110 \times 110 \times 35$ mm is formed in 3 stages. The initial wall angle is taken as process parameter, and at each stage wall angle is increased by 5° [41]. For example with a '0' level of initial wall angle, 50°, 55° and 60° degree wall is formed in first, second and third stage, respectively, as shown in Fig. 3. To form each stage, spiral tool path is used since it does not generate vertical tool markings on parts. The tool path for CNC milling machine is generated using 'CTIA V5R21' (developed by Dassault systems, France) and 'MATLAB 2020a' (developed by MathWorks, USA) [42].

All experiments are performed on Siemens controller CNC milling machine (Make: Batliboi Ltd, Surat, India). A fixture is designed and fabricated to hold sheet blank during

Table 1 Process parameters and their levels

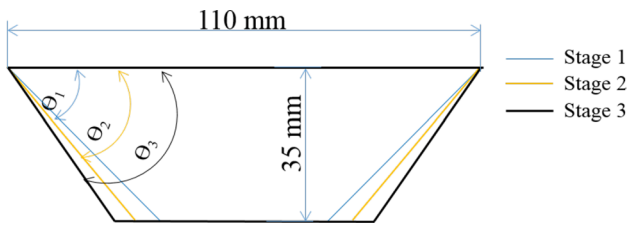| Parameters	Levels		
	-1	0	$+1$
Step depth (mm)	0.5	0.75	1
Tool diameter (mm)	12	14	16
Sheet thickness (mm)	1	1.5	2
Initial wall angle (°)	45	50	55

Fig. 3 Variation of wall angle per stage

the experiments. Blank is clamped using top plate and bottom plate as shown in Fig. 4.

The part formed by MSPIF process for experiment number 30 is shown in Fig. 5a. The geometry of part is square pyramid of size 110 mm × 110 mm with final wall angle of 55° and forming depth of 35 mm. Tool used for experiment is hemispherical with tip diameter of 12 mm as depicted in Fig. 5b.

For the present study, part thinning and peak forming force are taken as responses. Percentage thinning is calculated using following formula [Eq. (6)].

Fig. 4 Holding fixture on machine bed

Fig. 5 **a** Formed part and **b** hemispherical forming tool
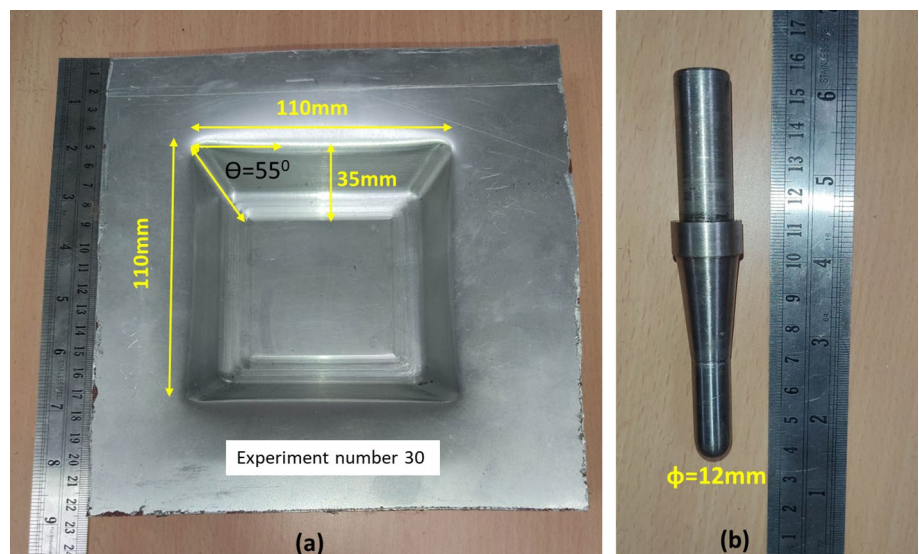
$$\text{Maximum thinning (\%)} = \frac{t_0 - t_{min}}{t_0} \times 100 \qquad (6)$$

where t_0 = initial sheet thickness, t_{min} = minimum thickness of part.

To measure t_{min}, parts were cut into two sections and thickness reading is taken using pointed digital micrometer (Make: Mitutoyo, Japan) at 5-mm intervals along depth as shown in Fig. 6.

Three components of forming force acting on blank during MSPIF process are depicted in Fig. 7. Vertical component of forming force [$F_{(z\text{-}max)}$] is the maximum or peak force acting on blank. Therefore, in the present work, $F_{(z\text{-}max)}$ is considered as one of the responses. To measure $F_{(z\text{-}max)}$, milling tool dynamometer (Make: Syscon Instruments Ltd. Bangalore, India) is fitted on machine bed. The base plate of fixture is placed over the dynamometer. The $F_{(z\text{-}max)}$ is noted from data acquisition system of milling tool dynamometer. Dynamometer gives the force reading in 'Kgf' unit. It is then converted into 'Newton (N)' by multiplying 9.806.

3 Results and discussion

The design layout for four-factor three-level CCD method and measured values of responses is given in Table 2. The minimum and maximum values of thinning are 56.80% and 77.50%, respectively, while 627.76 N and 2501.24 N are the minimum and maximum values of $F_{(z\text{-}max)}$, respectively. Analysis of variance (ANOVA) is performed to determine the significance of process parameters on the responses. The confidence interval for the study is considered as 95%;
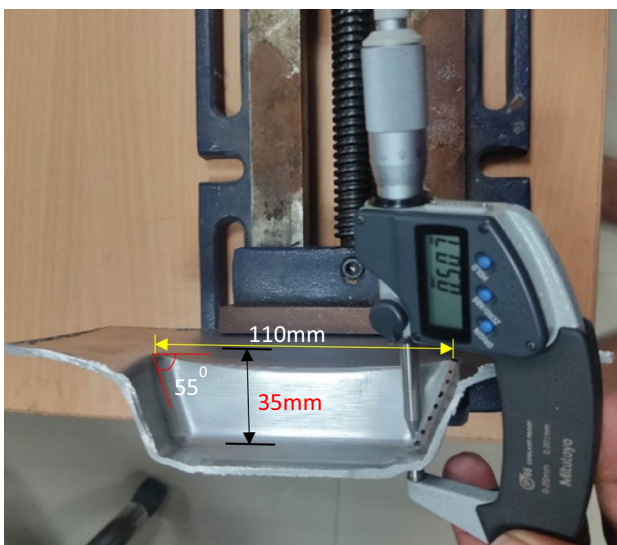

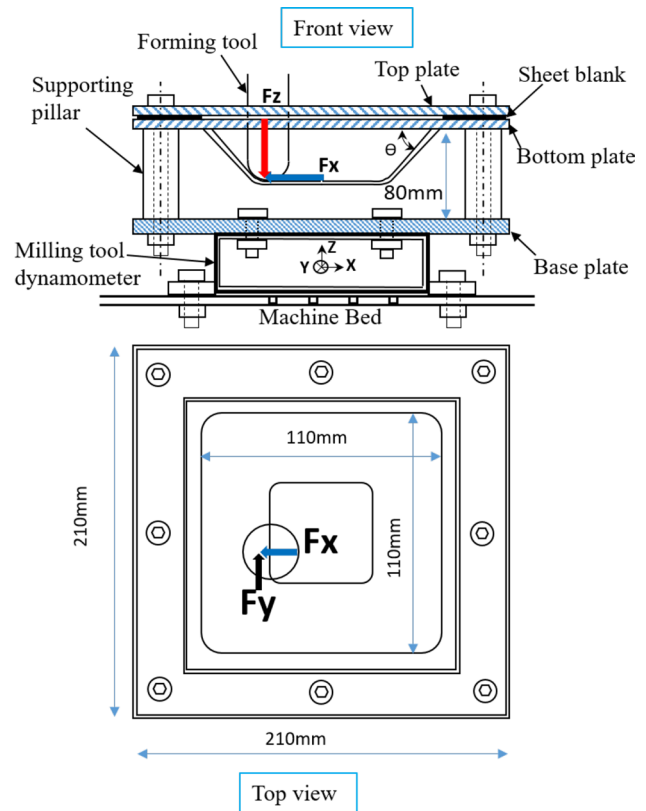**Fig. 6** Thickness measurement using digital micrometer

Fig. 7 Different components of forming force

therefore, the terms whose p value is less than 5% (i.e., 0.05) are significant terms. To validate the ANOVA, p value of 'lack of fit' term must be greater than 0.05 and implies the lack of fit is insignificant and the ANOVA model is significant. Signal to noise (SN) ratio must be greater than 4 to represent adequacy of the design space. The R^2 analysis is used to determine robustness of ANOVA model; the value closed to 1 indicates ANOVA model is mathematically valid.

3.1 Thinning of parts

Wall thickness distribution of a part formed by MSPIF process is shown in Fig. 8. The graph is plotted with respect to forming depth. It is observed that wall thickness is continuously decreasing with increase in forming depth. In most of cases, the minimum thickness is found at bottom corner points of pyramidal frustum. This is due to bi-axial stretching at corner points. As per sine law of thinning, the value of wall thickness is 0.5 mm (for $\theta = 60°$ and $t_0 = 1$ mm), while minimum thickness observed for the same setting is 0.336 mm.

ANOVA for thinning is given in Table 3. The value of R^2, R^2 (adj.) and R^2 (pred.) is 0.9779, 0.9575, and 0.8511, respectively. The SN ratio is 22.840; hence, the ANOVA model is used to navigate design space. From ANOVA, it is

Table 2 Experimental design and values of responses

Test run	Step depth (mm)	Tool diameter (mm)	Sheet thickness (mm)	Initial wall angle (°)	Thinning (%)	F_(z-max) (N)
1	0.75	14	1.5	50	69.3	1383.04
2	0.75	14	1.5	45	64.4	1320.65
3	1	12	2	55	71.9	2157.94
4	1	12	1	55	77.5	784.704
5	0.5	12	2	45	56.8	1716.54
6	0.5	12	2	55	72.2	1922.52
7	0.5	16	1	45	65.7	745.469
8	0.5	12	1	45	61.7	627.763
9	0.75	14	1.5	50	69.3	1353.61
10	1	12	2	45	59.2	1971.57
11	0.75	12	1.5	50	68.7	1324.19
12	0.75	14	1.5	50	69.3	1353.61
13	0.75	14	1.5	50	69.3	1392.85
14	1	14	1.5	50	67.9	1520.36
15	1	16	2	55	71.1	2501.24
16	0.75	14	1.5	55	74.7	1373.23
17	0.75	14	2	50	66.7	2059.85
18	1	12	1	45	62.3	696.425
19	0.75	14	1	50	69.4	804.322
20	1	16	2	45	57.7	2324.69
21	0.75	16	1.5	50	68.7	1539.98
22	0.75	14	1.5	50	69.3	1353.61
23	0.5	12	1	55	77	680.11
24	0.75	14	1.5	50	69.3	1373.23
25	0.5	14	1.5	50	70.3	1294.76
26	1	16	1	45	61.2	872.983
27	0.5	16	1	55	75	850.61
28	0.5	16	2	45	57.5	2001.12
29	0.5	16	2	55	72.5	2138.32
30	1	16	1	55	75.4	900.32

Fig. 8 Thickness distribution curve
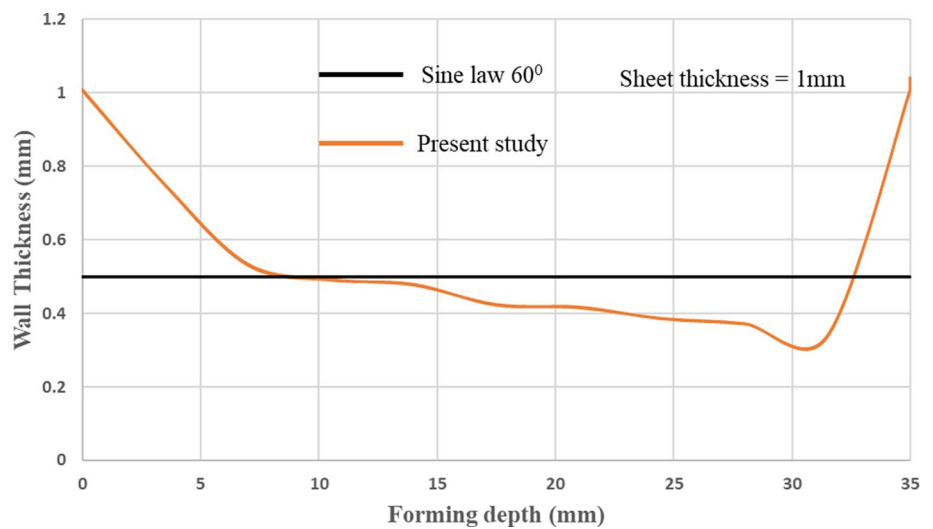
Table 3 ANOVA table for thinning

Source	Sum of squares	Degrees of freedom	Mean square	F value	p value	Remark
Model	937.29	14	66.95	47.32	<0.0001	Significant
A-step depth	1.13	1	1.13	0.7952	0.3866	
B-tool diameter	0.3472	1	0.3472	0.2454	0.6275	
C-sheet thickness	87.12	1	87.12	61.58	<0.0001	Significant
D-initial wall angle	810.7	1	810.7	573.02	<0.0001	Significant
AB	4.52	1	4.52	3.19	0.0942	
AC	0.9506	1	0.9506	0.6719	0.4252	
AD	0.0156	1	0.0156	0.011	0.9177	
BC	0.0006	1	0.0006	0.0004	0.9835	
BD	2.81	1	2.81	1.98	0.1795	
CD	0.3906	1	0.3906	0.2761	0.607	
A^2	0.2224	1	0.2224	0.1572	0.6973	
B^2	1.24	1	1.24	0.8794	0.3632	
C^2	4.67	1	4.67	3.3	0.0892	
D^2	0.0639	1	0.0639	0.0451	0.8346	
Residual	21.22	15	1.41			

found that initial wall angle and sheet thickness are significant process parameter for thinning. Moreover, no interaction is found significant in the study.

3.1.1 Main effect plot for thinning

Main effect plot of parameters on thinning is plotted at the center level (i.e., 0 level) in the design space as shown in Fig. 10. It is observed that thinning decreases with increase in sheet thickness (Fig. 10c) (similar results were obtained by Yang [43] for SPIF process). This is because increase in sheet thickness, stiffness of the sheet increases. Further, at larger sheet thickness, more material is available for next stage. This material opposes RBM; thus, thinning reduces. Therefore, to reduce sheet thinning, higher sheet thickness is preferable.

The thinning ratio (t_f/t_o) of material affects the strength and quality of formed parts, and initial sheet thickness has major impact on thinning ratio. To get uniformity in material flow, it is required to control the thinning ratio by increasing thickness of base material. The line graph of minimum and maximum thinning ratio for selected level of sheet thickness is shown in Fig. 9. It is found that both minimum and maximum thinning ratio for 2 mm sheet thickness is higher than the corresponding thinning ratio for 1 mm and 1.5 mm. Therefore, higher value of t_{min} is obtained with large value of sheet thickness.

It is also found that sheet thinning increases with increase in initial wall angle as depicted in Fig. 10d. The initial stage of MSPIF process is similar to SPIF. As per sine law [$t_f = t_0$ sin (90-θ)] of SPIF process, final wall thickness reduces with increase in wall angle. Thus, after first stage, less material is

available for subsequent stages. Therefore, stretching in all stages increases which results in increased thinning. Similar results were reported by Oleksik et al. [44] for SPIF process. As sheet thickness changes from 1 to 2 mm, there is 6.25% decrease in thinning, while initial wall angle changes from 45° to 55°, 21.37% increase in thinning is observed. It means wall angle has higher influence than sheet thickness. Moreover, large value of sheet thickness and low value of initial wall angle are required to reduce sheet thinning.

3.2 Vertical component of forming force (F_(z-max))

Large amount of F_(z-max) acts on the sheet material. These forces create strain hardening effect in MSPIF process. The principal strain distribution with respect to varying forming depth is shown in Fig. 11. Principal strain increases with increase in forming depth. It is noted that strain hardening effect is observed in range of 1.5–2.5 with corresponding depth range of 7–32 mm. Similar trend is also found by Kumar et al. [37].

The ANOVA for F_(z-max) is given in Table 4. The value of R^2, R^2 (Adj.) and R^2 (Pred.) is 0.9984, 0.9970 and 0.9917, respectively. The SN ratio is 88.63 and P-value of lack of fit is greater than 0.05; hence, the ANOVA model is used to navigate the design space. From ANOVA, all four process parameters are found significant for F_(z-max). Moreover, AC, BC and CD interactions are significant on F_(z-max).

3.2.1 Main effect plot for F_(z-max)

The main effect plot of process parameters on F_(z-max) is shown in Fig. 12. The graphs are plotted by keeping rest

Fig. 9 Thinning ratio variation
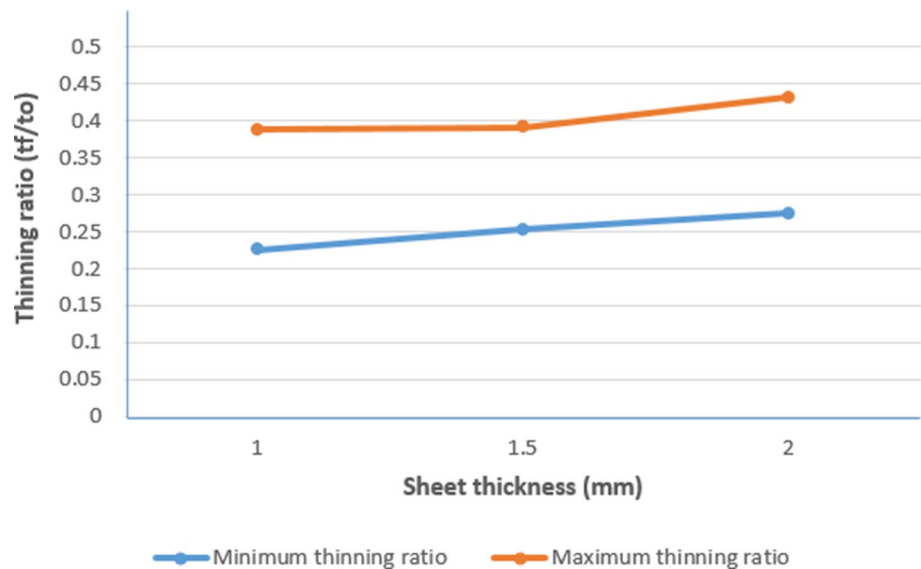
of parameters at mid-levels. From Fig. 12a, it is observed that F_(z-max) slightly increases with increase in step depth. With increased step depth, tool traverses at higher vertical distance. Thus, more material is stretched when the lattice plane is exposed to higher shear stress. As a result, more deforming energy is required to form part and hence F_(z-max) increases. Similar results have been reported by [33] al. for SPIF process. As the value of step depth changes from 0.5 to 1 mm, there is 15% (1298.54 N to 1493.31 N) increase in F_(z-max). From Fig. 12b, it is observed that F_(z-max) marginally increases with increase in tool diameter. This is because, with increase in tool diameter, contact area at tool–sheet interface increases and more material is deformed. Moreover, with larger contact area, sheet surface is affected by frictional force. Due to this more deformation energy is required; as a result, F_(z-max) increases. Similar results were obtained by Aerense et al.; Kumar and Gulati [32, 45] for SPIF. There is 16.29% (1324.19 N–1539.98 N) increase in F_(z-max) as tool diameter increases from 12 to 16 mm. It is also noted that F_(z-max) substantially increases with increase in sheet thickness (Fig. 12c). This is because, with increase in sheet thickness, more material per stage is available for forming and it requires higher deformation energy to form specific shape; therefore, larger forming force is required [34, 46]. With increase in sheet thickness from 1 to 2 mm, there is 170% (769.33 N–2077.73 N) increase in F_(z-max). It is also observed that with increase in initial wall angle, F_(z-max) increases slightly as shown in Fig. 12d. This is due to the fact that the larger amount of material has to be formed in a single contour for higher wall angle. Also, at higher initial wall angle, more lateral area of tool touches the sheet. The area at tool–blank interface is increased which requires more deformation energy; as a result, forming force increases. Similar results for SPIF were

obtained by Al-ghamdi et al.; Kumar et al. [36, 47]. The F_(z-max) increases with 8.97% (1277.97 N–1392.62 N) by increasing the initial wall angle from 45° to 55°.

3.2.2 Response surface plots of interactions for F_(z-max)

It is observed from the ANOVA as given in Table 4 that three interactions are found significant on F_(z-max) of MSPIF process. The combined effect of two parameters is investigated with 3-D response surface graph by keeping other parameters at middle level. The response surface plots for interactive process parameters are shown in Fig. 13.

The response surface plot of interaction for step depth and sheet thickness is shown in Fig. 13a, b. The F_(z-max) increases rapidly with combined increase in step depth and sheet thickness. The maximum value of F_(z-max) is observed at 1 mm step depth and 2 mm sheet thickness. At 1.5 mm sheet thickness, value of F_(z-max) increased by 17% (1298.54–1520.36 N) with increase in step depth from 0.5 mm to 1 mm, whereas at 0.75 mm step depth, F_(z-max) increased by 172.25% (763.16–2077.73 N) with increase in sheet thickness, proving that sheet thickness has greater impact on F_(z-max) than step depth. Also the contour lines are nearly parallel with axis of step depth. It means there is more impact of sheet thickness than step depth. From interaction graph, it is also inferred that F_(z-max) is more sensitive to change in sheet thickness than change in step depth. Lower value of step depth and sheet thickness is favorable to reduce F_(z-max). The response surface plot of interaction for tool diameter and sheet thickness is depicted in Fig. 13c, d. It is noted that value of F_(z-max) increases linearly with simultaneous increase in tool diameter and sheet thickness. Maximum value of F_(z-max) is observed at upper right corner of

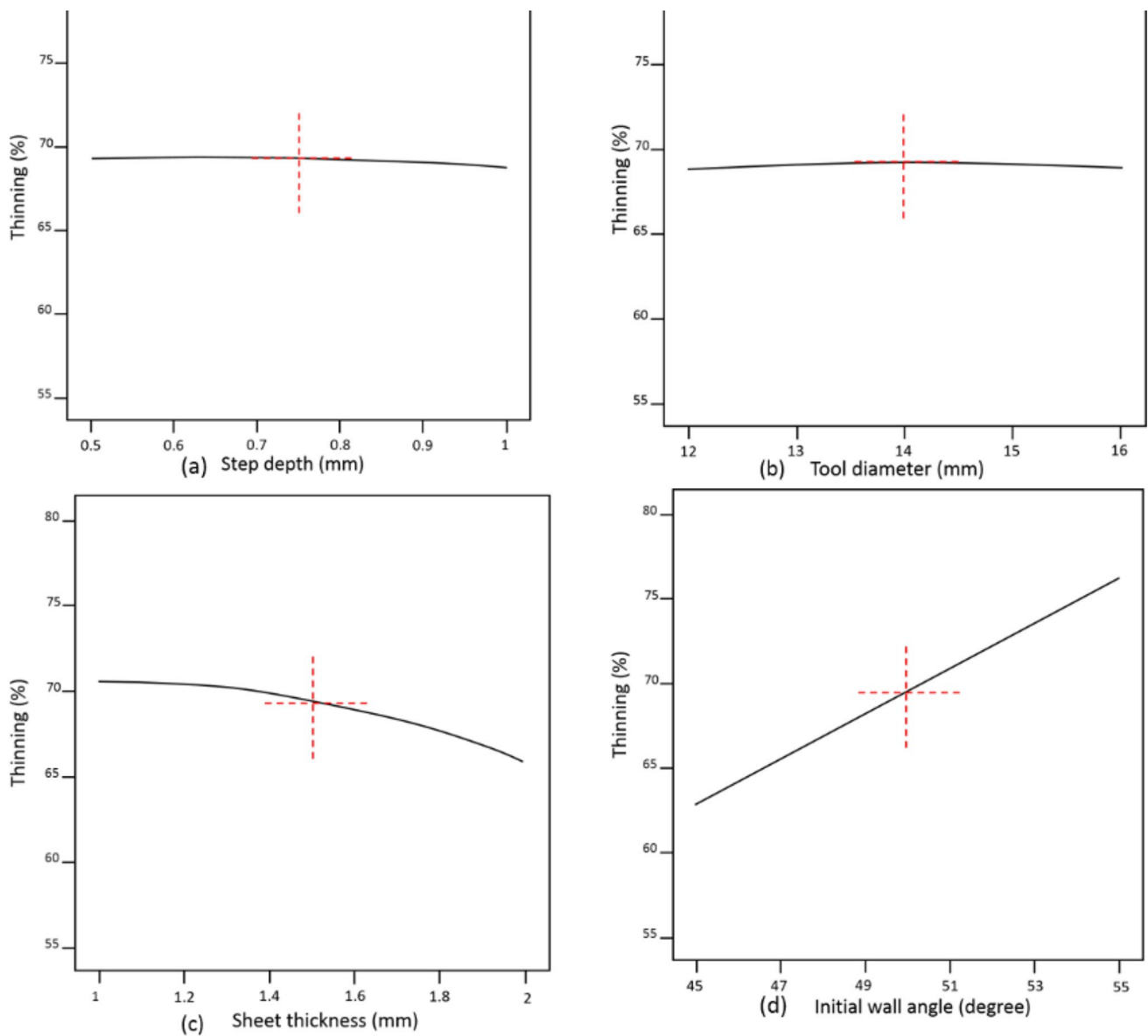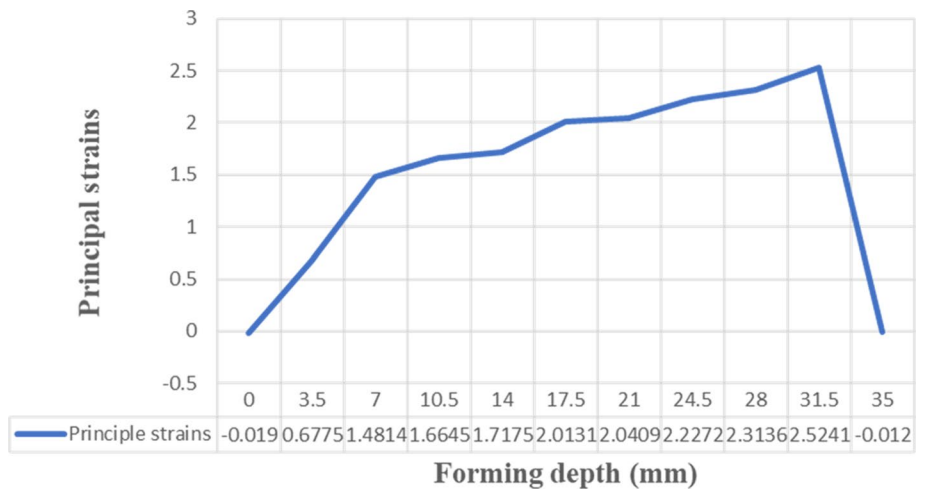**Fig. 10** Main effect plot of all parameters for thinning

Fig. 11 Strain distribution

	0	3.5	7	10.5	14	17.5	21	24.5	28	31.5	35
Principle strains	-0.019	0.6775	1.4814	1.6645	1.7175	2.0131	2.0409	2.2272	2.3136	2.5241	-0.012

Forming depth (mm)

Table 4 ANOVA table for peak vertical force

Source	Sum of squares	Degrees of freedom	Mean square	F value	p value	Remark
Model	8.33E+06	14	5.95E+05	686.49	<0.0001	Significant
A-step depth	1.71E+05	1	1.71E+05	196.9	<0.0001	Significant
B-tool diameter	2.21E+05	1	2.21E+05	254.49	<0.0001	Significant
C-sheet thickness	7.78E+06	1	7.78E+06	8968.53	<0.0001	Significant
D-initial wall angle	59,144.47	1	59,144.47	68.21	<0.0001	Significant
AB	2500.5	1	2500.5	2.88	0.1101	
AC	42,688.85	1	42,688.85	49.23	<0.0001	Significant
AD	30.61	1	30.61	0.0353	0.8535	
BC	23,748.23	1	23,748.23	27.39	0.0001	Significant
BD	470.27	1	470.27	0.5424	0.4728	
CD	11,718.32	1	11,718.32	13.51	0.0022	Significant
A^2	659.9	1	659.9	0.7611	0.3967	
B^2	4245.81	1	4245.81	4.9	0.0428	
C^2	4245.81	1	4245.81	4.9	0.0428	
D^2	5168.19	1	5168.19	5.96	0.0275	
Residual	13,006.08	15	867.07			
Lack of fit	11,514.79	10	1151.48	3.86	0.0745	Not significant
Pure error	1491.29	5	298.26			
Total	8.35E+06	29				

the graph. From interaction graph it is also observed that sheet thickness is more sensitive toward change in $F_{(z-max)}$ than tool diameter. At 1.5 mm sheet thickness, $F_{(z-max)}$ increased by 16.92% (1309.73–1531.17N) with increase in tool diameter from 12 to 16 mm. However, at 14 mm tool diameter, $F_{(z-max)}$ increased by 172.25% (763.165–2077.73 N) with increase in sheet thickness from 1 to 2 mm, which validates that sheet thickness has greater impact on $F_{(z-max)}$ than tool diameter. The contour lines are parallel to axis of tool diameter; therefore, it is inferred that small tool diameter combined with lower sheet thickness, reduces $F_{(z-max)}$ in MSPIF process. Response surface plot of interaction for sheet thickness and initial wall angle is shown in Fig. 13e, f. The $F_{(z-max)}$ increases rapidly with simultaneous increase in sheet thickness and initial wall angle. The contour lines are parallel to axis of initial wall angle; hence, it reveals that sheet thickness has larger effect on $F_{(z-max)}$ of MPSIF process. In addition, at 1.5 mm sheet thickness, value of $F_{(z-max)}$ increased by 8.97% (1277.98 N to 1392.62 N) with increasing initial wall angle from 45° to 55°, while, at 50° initial wall angle, $F_{(z-max)}$ increased by 172.82% (760.16–2073.93 N). It is inferred that low value of initial wall angle and lower sheet thickness minimizes the value of $F_{(z-max)}$.

From experimental study, it is revealed that sheet thickness is the most influencing factor on $F_{(z-max)}$ followed by tool diameter, step depth and initial wall angle.

4 Regression models

ANOVA suggested that regression models of responses are well defined by quadratic equation. It contains all terms which effects on selected responses. The regression models in terms of actual factors for percentage thinning and $F_{(z-max)}$ are given in Table 5. The terms in regression models are used to predict the responses for given levels of each process parameter for selected range. The levels should be specified in original units. These regression models are only valid for the selected material (i.e., aluminum 3003 alloy). The R^2 (pred.) indicates how well a regression model predicts the response. In the present study, R^2 (pred.) for thinning (%) and $F_{(z-max)}$ (N) are 0.8511 and 0.9917, respectively, which is close to 1 and hence these regression models are accepted. Equation (7) and Eq. (8) are the regression models for thinning (%) and $F_{(z-max)}$ (N), respectively.

From Eq. (7), it is noted that all process parameters (i.e., step depth, tool diameter, sheet thickness and initial wall angle) have undesired effect on thinning, while, from Eq. (8), it is clear that initial wall angle has favorable effect and step depth, tool diameter and sheet thickness have unfavorable effect on $F_{(z-max)}$. The plot of predicted and actual responses for thinning and $F_{(z-max)}$ is shown in Fig. 14a and b, respectively. It is observed that data points are distributed along the straight line proving predictive and experimental values are in good agreement.
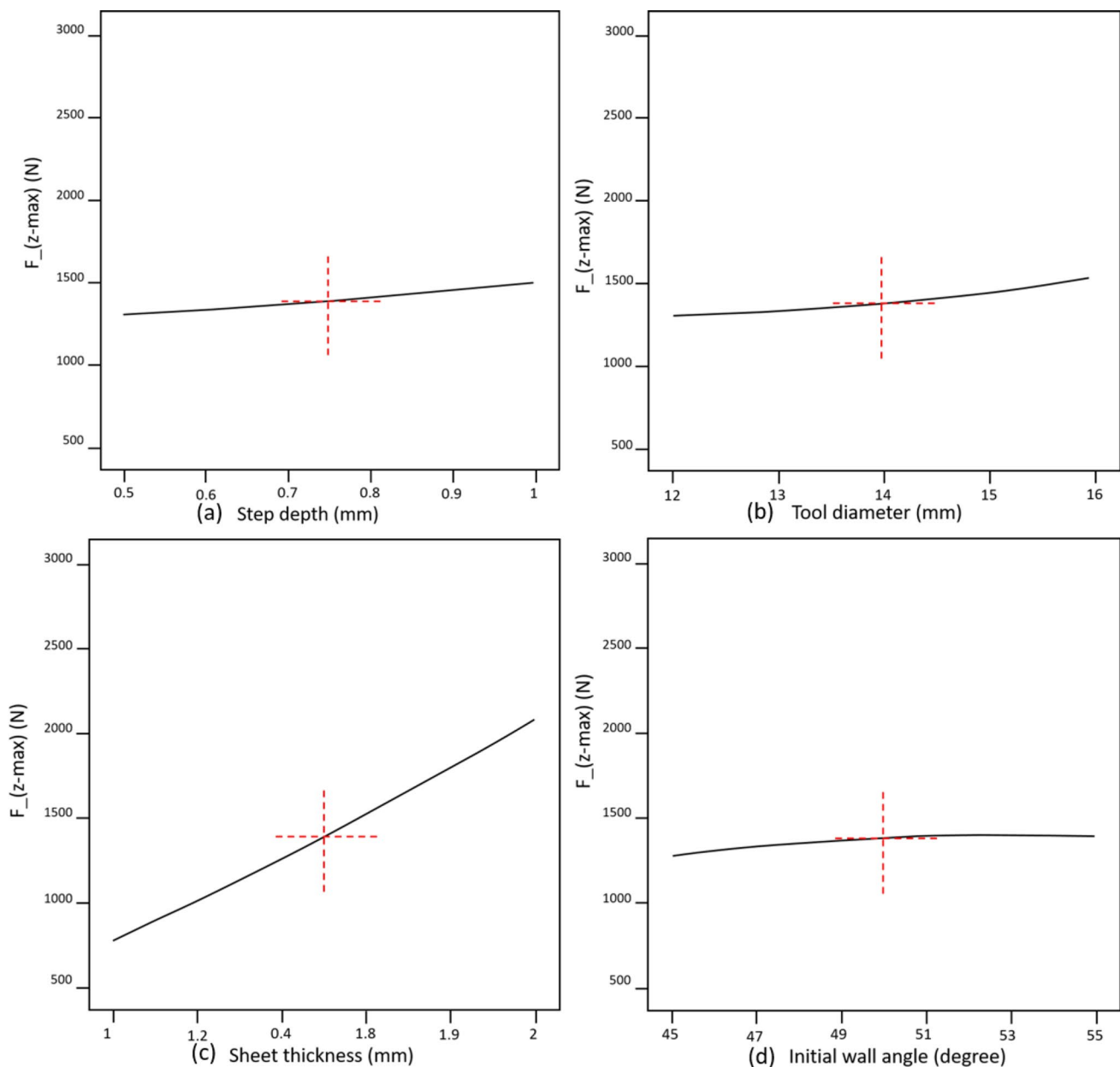
Fig. 12 Main effect plot of all parameters for F_(z-max)

5 Optimization

From experimental data (Table 2), the minimum value of thinning (56.8%) is obtained at test run number 5, whereas minimum value of F_(z-max) (627.76 N) is obtained at test run number 7. These test runs have different levels of process parameters. If test run number 5 is performed though it results in minimum thinning, but corresponding value of F_(z-max) is not minimum. Similar results observed with test number 8. The present study is focused to minimize both responses simultaneously. Therefore, multi-objective optimization of process parameters is performed to minimize

thinning and F_(z-max) simultaneously. Using desirability approach, both responses are grouped in desirability function and bounded by 0 to 1, where 1 is desired and 0 is undesired response. The desirability of response is obtained from the literature (Khuri, Aksezer [48, 49]). The optimized level of step depth, tool diameter, sheet thickness and initial wall angle is obtained, which simultaneously satisfies the optimization criteria given in Table 6. The optimized levels of selected process parameters are—(i) step depth—0.5 mm, (ii) tool diameter—12 mm, (iii) sheet thickness—1 mm, (iv) 45° initial wall angle—45^0. From results, the optimized percentage of thinning is observed as 62.52%, the
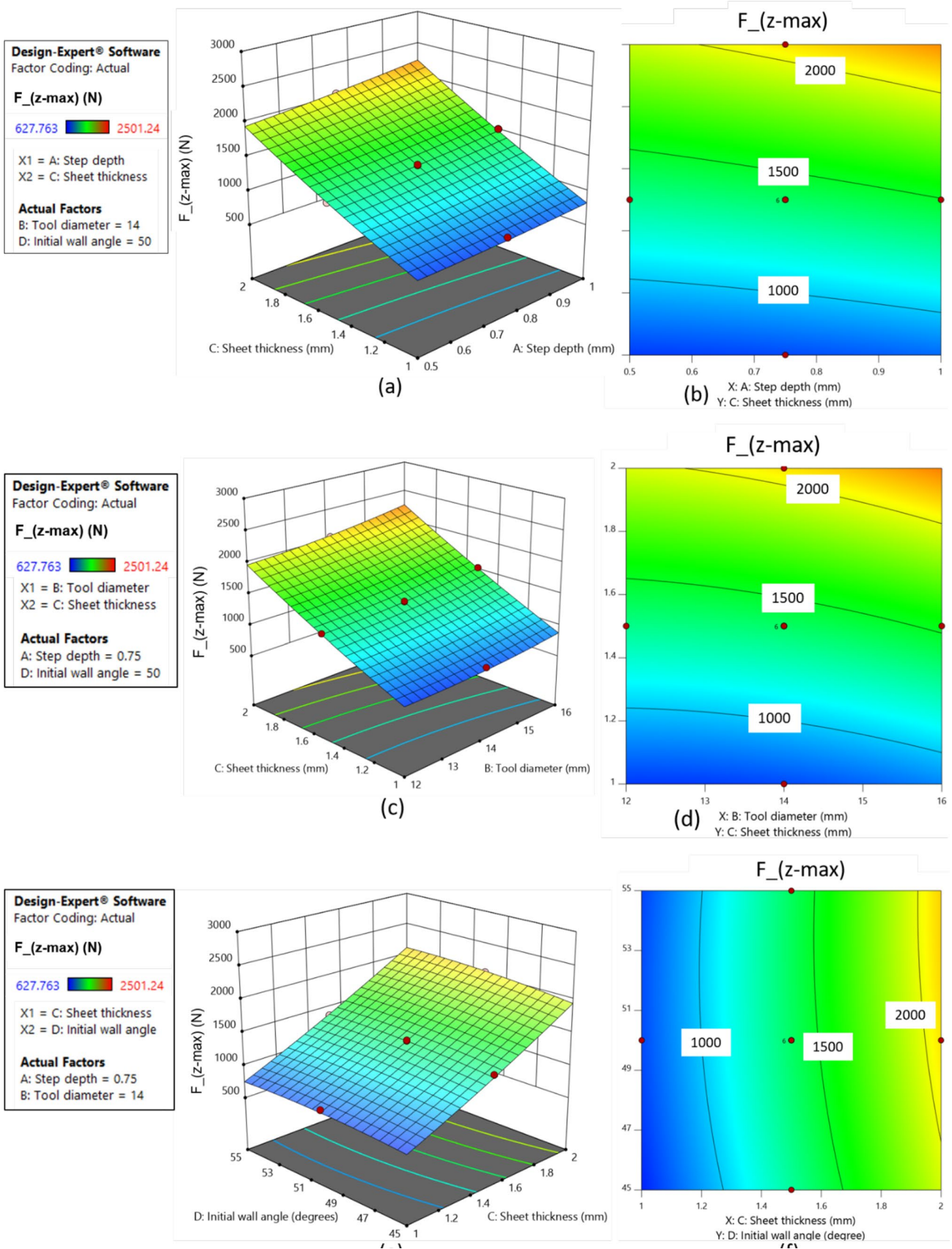
Fig. 13 Response surface plot for F_(z-max)

Table 5 Regression models for responses

Response	Regression model	Equation
Thinning (%)	$-55 + 16.73 \times (A) + 7.68 \times (B) + 7.21 \times (C) + 1.18 \times (D) - 1.06 \times (A) \times (B) + 1.95 \times (A) \times (C) + 0.025 \times (A) \times (D) - 0.00625 \times (B) \times (C) - 0.04 \times (B) \times (D) + 0.0625 \times (C) \times (D) - 4.68 \times (A^2) - 0.173 \times (B^2) - 5.37 \times (C^2) + 0.006 \times (D^2)$	(7)
F_(z-max) (N)	$-2279.67 - 908.01 \times (A) - 277.44 \times (B) - 561.75 \times (C) + 182.29 \times (D) + 25.00 \times (A) \times (B) + 413.22 \times (A) \times (C) - 1.10 \times (A) \times (D) + 38.52 \times (B) \times (C) - 0.54 \times (B) \times (D) + 10.82 \times (C) \times (D) + 255.34 \times (A^2) + 10.120 \times (B^2) + 161.92 \times (C^2) - 1.78 \times (D^2)$	(8)

corresponding thickness ratio is 0.3748 with initial thickness of 1 mm, and optimized value of F_(z-max) is 632.44 N. With optimized levels, there is 10.07% and 0.745% change in thinning and F_(z-max), respectively.

The desirability change with respect to selected process parameter is shown in Fig. 15. The graph shows that more acceptable results are occurred at 0.5 mm step depth and 12 mm tool diameter. Least acceptance occurs at 16 mm tool with 0.5 mm step depth.

Desirability factor is the percentage difference in optimized value and observed value (minimum in this case). Bar chart of desirability for process parameters with responses is depicted in Fig. 16. The values of desirability of thinning and F_(z-max) are 0.9974 and 0.7233, and the combined desirability of both responses is 0.849. The maximum value of the factor is desirable for the selected criteria. Number of optimized solutions are obtained based on desirability change in both responses. Solution with maximum combined desirability has been
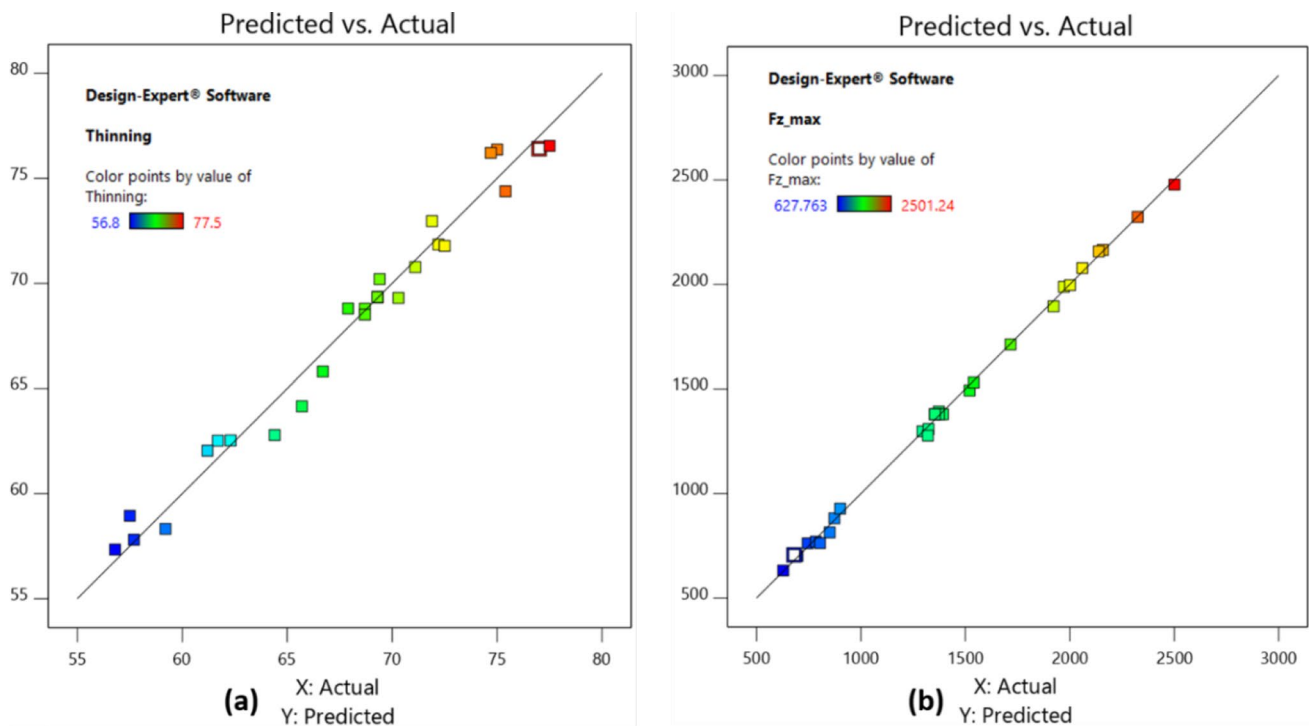
Fig. 14 Predicted versus actual values of **a** thinning and **b** F_(z-max)

Table 6 Optimization criteria and results

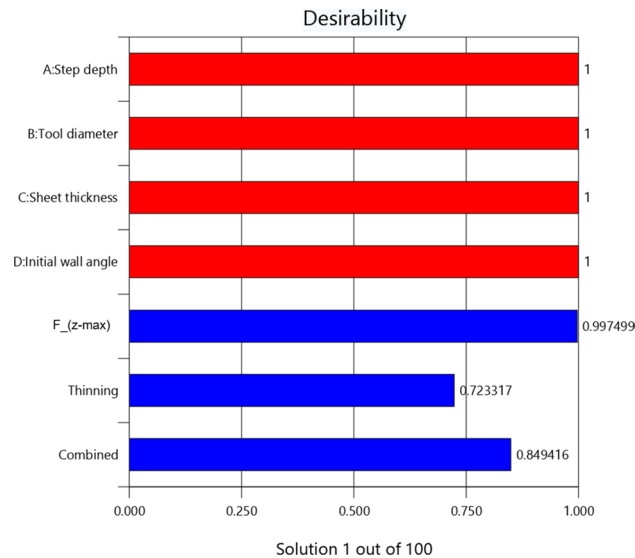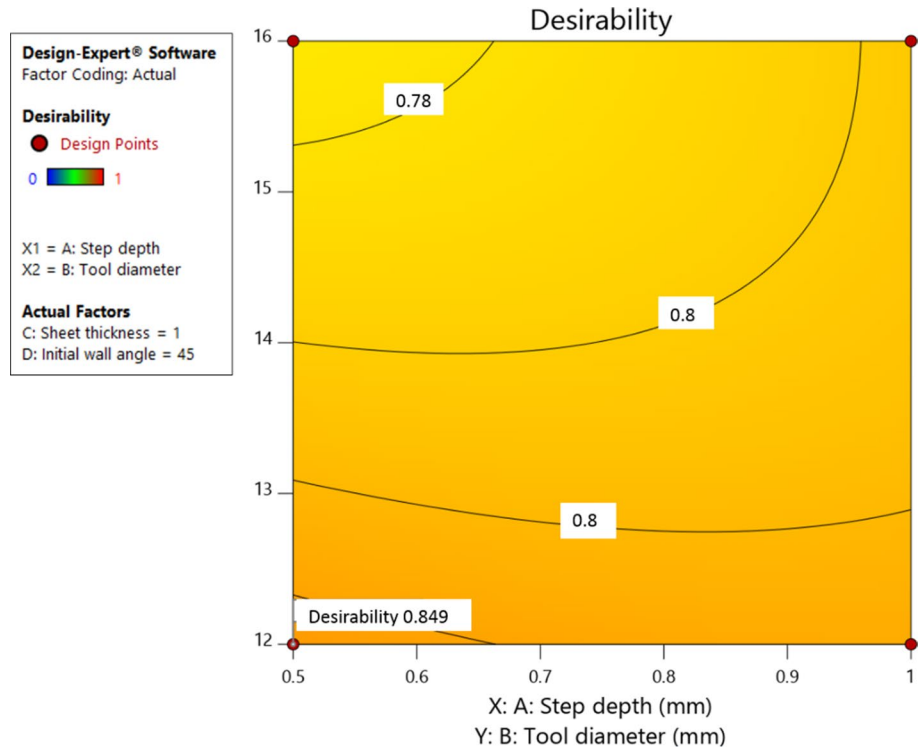| S.no.	Factors	Criteria	Lower limit	Upper limit	Optimized value
1	Step depth (mm)	In range	0.5	1	0.5
2	Tool diameter (mm)	In range	12	16	12
3	Sheet thickness (mm)	In range	1	2	1
4	Initial wall angle (°)	In range	45	55	45
5	Thinning (%)	Minimize	56.8	77.5	62.52
6	F_(z-max) (N)	Minimize	627.76	2501.24	632.44

Fig. 15 Desirability graph

Fig. 16 Bar chart of desirability

chosen for the study. Moreover, the accuracy of F_(z-max) model is more than thinning model; hence, more weightage is given to F_(z-max).

6 Confirmation tests

To validate the results of regression model and optimized values of process parameters, confirmation tests are performed. Three tests are performed to validate the results of regression model of thinning and F_(z-max). Four experiments are performed to validate optimization results [50]. The deviation (%) is calculated using Eq. (9).

$$\text{Deviation}\,(\%) = \frac{|\text{Predicted value} - \text{Actual value}|}{\text{Predicted value}} \times 100$$

(9)

The results of confirmation tests are given in Tables 7 and 8. The average deviation for both confirmation tests is less than 10%, and therefore, results are accepted.

7 Conclusion

The present paper describes an experimental investigation on part thinning and peak forming force (F_(z-max)) acting in MSPIF process. Experiments are designed using CCD method and analyzed using ANOVA. Quadratic regression models are developed to predict the value of responses. Next, multi-objective optimization of process parameter is performed using desirability approach. The key findings of present work are as follows:

Table 7 Confirmation test results for regression models

S.N	Process parameters				Responses					
	Step depth (mm)	Tool diameter (mm)	Sheet thickness (mm)	Initial wall angle (°)	Thinning			F_(z-max)		
					Predicted (%)	Actual (%)	Deviation (%)	Predicted (N)	Actual (N)	Deviation (%)
1	0.6	12	1.2	48	66.65	68.25	2.39	900.37	828.11	8.02
2	0.75	15	1.5	50	69.10	65.47	5.25	1445.45	1402.37	2.98
3	0.85	16	2	52	67.31	63.25	6.03	2358.58	2481.71	5.20

Table 8 Confirmation test results of optimized values

S.N	Thinning			F_(z-max)		
	Predicted (%)	Actual (%)	Deviation (%)	Predicted (%)	Actual (%)	Deviation (%)
1	62.52	63.25	1.15	632.45	610.13	3.53
2	62.52	62.13	0.96	632.45	613.45	3.00
3	62.52	63.18	1.04	632.45	630.94	0.238
4	62.52	63.24	1.14	632.45	624.68	1.23
Average deviation (%)			1.07			2.05

(i) It is found that initial wall angle and sheet thickness are significant process parameters for thinning of parts formed with MSPIF process. Initial wall angle has more influence than sheet thickness. Also, no interaction effect is found significant for thinning. Thinning reduces with decrease in initial wall angle and increase in sheet thickness. The minimum and maximum thinning ratio (t_f/t_0) in case of sheet thickness of 2 mm is higher than 1 mm and 1.5 mm. Therefore, higher value of t_{min} is obtained with large value of sheet thickness.

(ii) For F_(z-max), all process parameters, namely, step depth, tool diameter, sheet thickness and initial wall angle, are found significant. Also, the interaction effect of step depth-sheet thickness, tool diameter-sheet thickness and wall angle-sheet thickness is found significant. Sheet thickness is the most significant process parameter followed by tool diameter, step depth and initial wall angle. F_(z-max) decreases with decrease in level of all four parameters. The strain hardening effect is also observed due to large forming forces. Principal strain increases with increase in forming depth. Strain hardening occurred in range of 1.5–2.5 strain value with corresponding depth range of 7–32 mm

(iii) Quadratic regression model gives best fit with 95% confidence level for both responses. The regression models are validated using confirmation test. The results are within acceptable range.

(iv) The optimized levels of selected process parameters are 0.5 mm step depth, 12 mm tool diameter, 1 mm sheet thickness and 45^0 initial wall angle. The corresponding optimized values of thinning and F_(z-max) are 62.52% and 634.44 N, respectively. The thinning ratio is 0.374 with 1 mm initial thickness. With process optimization, there are 10.07% and 0.745% change in thinning and F_(z-max), respectively (with 0.849 combined desirability), which is in acceptable range. Results are verified using confirmation tests.

The findings of this research are useful in efficient process planning of MSPIF process to improve quality of formed parts.

Declarations

Conflict of interest The corresponding author states that there is no conflict of interest on behalf of all authors.

References

1. Micari F, Ambrogio G, Filice L (2006) Shape and dimensional accuracy in single point incremental forming: state of the art and future trends. J Mater Process Technol 191:390–395

2. Li Y, Chen X, Liu Z, Sun J, Li F, Li J (2017) A review on the recent development of incremental sheet-forming process. Int J Adv Manuf Technol 92(5–8):2439–2462

3. Duflou JR, Verbert J, Belkassem B, Gu J, Sol H, Henrard C et al (2008) Process window enhancement for single point incremental forming through multi-step toolpaths. CIRP Ann-Manuf Technol 57(1):253–256

4. Vignesh G, Pandivelan C, Sathiya Narayanan C (2019) Review on multi-stage incremental forming process to form vertical walled cup. Mater Today Pro 27:2297–2302

5. Shi X, Hussain G, Zha G, Wu M, Kong F (2014) Study on formability of vertical parts formed by multi-stage incremental forming. Int J Adv Manuf Technol 75(5–8):1049–1053

6. Liuru Z, Yinmei Z, Zhongmin L (2015) Study on forming method of vertical wall cylinder parts formed by multi-stage incremental forming. Mater Res Innov 19:6102–6104

7. Liuru Z, Yinmei Z (2015) A new method for multi-pass single-point incremental forming of vertical wall square box with small corner radius. Mater Res Innov 19:5543–5550

8. Kim TJ, Yang DY (2000) Improvement of formability for the incremental sheet metal forming process. Int J Mech Sci 42(7):1271–1286

9. Iseki H, Naganawa T (2002) Vertical wall surface forming of rectangular shell using multistage incremental forming with spherical and cylindrical rollers. J Mater Process Technol 130–131:675–679

10. Filice L (2006) A phenomenology-based approach for modelling material thinning and formability in incremental forming of cylindrical parts. Proc Inst Mech Eng Part B J Eng Manuf 220(9):1449–1455

11. Verbert J, Belkassem B, Henrard C, Habraken AM, Gu J, Sol H et al (2008) Multi-Step toolpath approach to overcome forming limitations in single point incremental forming. Int J Mater Form 1:1203–1206

12. Manco L, Filice L, Ambrogio G (2011) Analysis of the thickness distribution varying tool trajectory in single-point incremental forming. Proc Inst Mech Eng Part B J Eng Manuf 225(3):348–356

13. Li J, Hu J, Pan J, Geng P (2012) Thickness distribution and design of a multi-stage process for sheet metal incremental forming. Int J Adv Manuf Technol 62(9–12):981–988

14. Li J, Shen J, Wang B (2013) A multipass incremental sheet forming strategy of a car taillight bracket. Int J Adv Manuf Technol 69(9–12):2229–2236

15. Li J, Geng P, Shen J (2013) Numerical simulation and experimental investigation of multistage incremental sheet forming. Int J Adv Manuf Technol 68(9–12):2637–2644

16. Liu Z, Li Y, Meehan PA (2013) Vertical wall formation and material flow control for incremental sheet forming by revisiting multistage deformation path strategies. Mater Manuf Process 28(5):562–571

17. Cao T, Lu B, Xu D, Zhang H, Chen J, Long H et al (2015) An efficient method for thickness prediction in multi-pass incremental sheet forming. Int J Adv Manuf Technol 77(1–4):469–483

18. Moser N, Ndip-Agbor E, Ren H, Zhang Z, Ehmann K, Cao J (2015) Challenges and process strategies concerning multi-pass double sided incremental forming. Key Eng Mater 651–653:1122–1127

19. Lingam R, Bansal A, Reddy NV (2016) Analytical prediction of formed geometry in multi-stage single point incremental forming. Int J Mater Form 9(3):395–404

20. Otsu M, Ogawa T, Muranaka T, Yoshimura H, Matsumoto R (2017) Improvement of forming limit and accuracy in friction stir incremental forming with multistage forming. Procedia Eng 207:807–812

21. Dai P, Chang Z, Li M, Chen J (2019) Reduction of geometric deviation by multi-pass incremental forming combined with tool path compensation for non-axisymmetric aluminum alloy component with stepped feature. Int J Adv Manuf Technol 102(1–4):809–817

22. Ndip-Agbor E, Cheng P, Moser N, Ehmann K, Cao J (2019) Prediction of rigid body motion in multi-pass single point incremental forming. J Mater Process Technol 269:117–127

23. Zhu H, Cheng G, Jung D (2021) Toolpath planning and generation for multi-stage incremental forming based on stretching angle. Materials (Basel). 14(17)

24. Gohil AM, Modi BA (2021) Multistage tool path strategy to produce hemispherical shape using single point incremental forming process. Int J Mechatron Manuf Syst 14(3–4):181–201

25. Ullah S, Li X, Xu P, Li D (2022) Experimental and numerical investigation for sheet thickness thinning in two-point incremental forming (TPIF). Int J Adv Manuf Technol 122(5–6):2493–2512

26. Malhotra R, Bhattacharya A, Kumar A, Reddy NV, Cao J (2011) A new methodology for multi-pass single point incremental forming with mixed toolpaths. CIRP Ann-Manuf Technol 60(1):323–326

27. Xu D, Malhotra R, Reddy NV, Chen J, Cao J (2012) Analytical prediction of stepped feature generation in multi-pass single point incremental forming. J Manuf Process 14(4):487–494

28. Nirala HK, Agrawal A (2018) Sheet thinning prediction and calculation in incremental sheet forming. Springer Singapore 391–410

29. Ambrogio G, Filice L, Micari F (2006) A force measuring based strategy for failure prevention in incremental forming. J Mater Process Technol 177(1–3):413–416

30. Duflou J, Tunçkol Y, Szekeres A, Vanherck P (2007) Experimental study on force measurements for single point incremental forming. J Mater Process Technol 189(1–3):65–72

31. Durante M, Formisano A, Langella A, Capece Minutolo FM (2009) The influence of tool rotation on an incremental forming process. J Mater Process Technol 209(9):4621–4626

32. Aerens R, Eyckens P, Van Bael A, Duflou JR (2010) Force prediction for single point incremental forming deduced from experimental and FEM observations. Int J Adv Manuf Technol 46(9–12):969–982

33. Liu Z, Li Y, Meehan PA (2013) Experimental investigation of mechanical properties, formability and force measurement for AA7075-O aluminum alloy sheets formed by incremental forming. Int J Precis Eng Manuf 14(11):1891–1899

34. Bagudanch I, Garcia-Romeu ML, Centeno G, Elías-Zúñiga A, Ciurana J (2015) Forming force and temperature effects on single point incremental forming of polyvinylchloride. J Mater Process Technol 219:221–229

35. Shrivastava P, Tandon P (2019) Effect of preheated microstructure vis-à-vis process parameters and characterization of orange peel in incremental forming of AA1050 sheets. J Mater Eng Perform 28(5):2530–2542

36. Kumar A, Gulati V (2018) Experimental investigations and optimization of forming force in incremental sheet forming. Sadhana Acad Proc Eng Sci 43(10):1–15

37. Kumar A, Gulati V, Kumar P (2018) Investigation of process variables on forming forces in incremental sheet forming. Int J Eng Technol 10(3):680–684

38. Gheysarian A, Honarpisheh M (2019) Process parameters optimization of the explosive-welded Al/Cu bimetal in the incremental sheet metal forming process. Iran J Sci Technol Trans Mech Eng 43(2013):945–956

39. Gandla PK, Inturi V, Kurra S, Radhika S (2020) Evaluation of surface roughness in incremental forming using image processing based methods. Meas J Int Meas Confed 164:108055

40. Liu Z, Daniel WJT, Li Y, Liu S, Meehan PA (2014) Multi-pass deformation design for incremental sheet forming: analytical modeling, finite element analysis and experimental validation. J Mater Process Technol 214(3):620–634

41. Cerro I, Maidagan E, Arana J, Rivero A, Rodríguez PP (2006) Theoretical and experimental analysis of the dieless incremental sheet forming process. J Mater Process Technol 177(1–3):404–408

42. Bari N, Kumar S (2022) Multi-stage single-point incremental forming: an experimental investigation of surface roughness and forming time. J Mater Eng Perform

43. Yang M, Yao Z, Li Y, Li P, Cui F, Bai L (2018) Study on thickness thinning ratio of the forming parts in single point incremental forming process. Adv Mater Sci Eng

44. Oleksik V (2014) Influence of geometrical parameters, wall angle and part shape on thickness reduction of single point incremental forming. Procedia Eng 81:2280–2285

45. Kumar A, Gulati V, Kumar P (2018) Investigation of process variables on forming forces in incremental sheet forming. Sadhana Acad Proc Eng Sci 10(3):1–15

46. Arfa H, Bahloul R, BelHadjSalah H (2013) Finite element modelling and experimental investigation of single point incremental forming process of aluminum sheets: Influence of process parameters on punch force monitoring and on mechanical and geometrical quality of parts. Int J Mater Form 6(4):483–510

47. Al-Ghamdi KA, Hussain G (2015) Forming forces in incremental forming of a geometry with corner feature: investigation into the effect of forming parameters using response surface approach. Int J Adv Manuf Technol 76(9–12):2185–2197

48. Khuri AI (2006) Response surface methodology and related topics. World scientific

49. Aksezer SC (2008) On the sensitivity of desirability functions for multiresponse optimization. J Ind Manag Optim 4(4):685–696

50. Jensen WA (2016) Confirmation runs in design of experiments. J Qual Technol 48(2):162–177